

Measurements of phase distortions through pulse characterization

GO Dwapanyin, GW Bosman, PH Neethling and EG Rohwer

Laser Research Institute, Physics Department, Stellenbosch University, Private bag X1, Matieland, 7602, South Africa

E-mail: 19724020@sun.ac.za

Abstract. The interaction of light with any material with refractive index, n , affects not only the amplitude of the transmitted light but also its phase. Accurate determination of the spectral phase of a laser pulse is paramount in various spectroscopic applications. There are many phase measurement techniques such as direct interferometric approaches including Frequency Resolved Optical Gating (FROG) and Spectral Phase Interferometry for Direct Electric-field Reconstruction (SPIDER) as well as indirect techniques such as ptychography. This work discusses an alternative approach of measuring phase distortions through the use of a Multiphoton Intrapulse Interference Phase Scan (MIIPS) and investigates the possibility of using MIIPS as a new complimentary phase contrast imaging technique. The principle of the technique as well as the determination of the group delay dispersion (GDD) of the generated signal is analysed and it's potential use in phase contrast imaging has also been identified.

1. Introduction

The propagation of a broadband ultrashort laser pulse through a dielectric medium results in the dispersion of the spectral components of the pulse due to the wavelength dependence of the refractive index n of the medium. The spectral components therefore travel with different speeds which may result in temporal pulse broadening and compression. More precisely, each of the spectral components of the pulse, propagating through a dispersive medium of length L will acquire a phase shift given by,

$$\phi(\omega) = k(\omega)L \quad (1)$$

here $k(\omega) = n(\omega)\omega/c$ is the frequency dependant propagation function, $n(\omega)$ the refractive index and c the speed of light. The functional dependence of phase shift, or rather the relative phase shift between the spectral components contained in the pulse, provides insight into how the pulse profile changes as it propagates through the medium. For the propagation of an ultrashort pulse through a dispersive medium, the velocity at which the pulse envelope propagates is of key importance. This velocity, known as the group velocity v_g , is defined as the inverse derivative of the propagation constant with respect to the angular frequency:

$$\frac{1}{v_g} = \frac{dk}{d\omega} = \frac{n}{c} + \frac{\partial n}{\partial \omega} \frac{\omega}{c} \quad (2)$$

For a dispersive medium where $\frac{\partial n}{\partial \omega} \neq 0$, the v_g therefore varies as the pulse propagates through the medium. To illustrate the influence this has on pulse propagation, it is customary to compute

the Taylor expansion of $k(\omega)$ about a central frequency ω_0 of the pulse

$$k = k_0 + k'(\omega - \omega_0) + \frac{k''}{2!}(\omega - \omega_0)^2 + \frac{k'''}{3!}(\omega - \omega_0)^3 + \dots \quad (3)$$

where (...) corresponds to higher order expansion terms. Substituting eqn.3 into eqn.1 gives a polynomial function of the order $\phi = \phi_0 + \phi' + \phi'' + \dots$ where it can be shown that $\phi_0 = k(\omega_0)L$ is related to the phase velocity of the pulse, $\phi' = k'(\omega - \omega_0)L$ relates to the group velocity of the pulse, $\phi'' = k''(\omega - \omega_0)^2L$ is the phase dispersion term where its coefficient, $k'' = \partial^2k/\partial\omega^2$, is the group velocity dispersion (GVD), whilst the GVD per unit length is the group delay dispersion (GDD). Note that the GVD is a purely medium dependent parameter. Furthermore, the GVD (or GDD) under specific circumstances is responsible for the temporal pulse broadening and compression [1].

There are many techniques to measure [1–3] and compensate for the phase shift between the spectral components of an ultrashort laser pulse. Compensation techniques includes the use of chirped mirrors [4], rotating cylindrical lens [5] and temporal pulse compression algorithms [6]. The phase distortion (dispersion) of a pulse can also be measured and corrected using an algorithm that combines both spectral phase characterization and compensation with temporal pulse compression in a single technique. This technique is Multiphoton Intrapulse Interference Phase Scan (MIIPS) [7].

2. Theory of MIIPS

MIIPS is a technique that permits the simultaneous measurement and shaping of femtosecond laser pulses. Unlike conventional pulse measurement techniques such as FROG [1], SPIDER [2] and background-free autocorrelation which measure only pulse characteristics, MIIPS can measure the characteristics as well as compress the pulse to a transform limited pulse. It entails the use of a $4f$ -shaper setup along with an iterative algorithm to measure the group delay dispersion (GDD) and to compensate for this measured phase distortion [8]. This is the fundamental advantage of MIIPS over FROG and SPIDER [9]. MIIPS works by introducing a guess phase as a reference phase function onto the 1D spatial light modulator that is in the $4f$ -shaper. This reference phase reduces or cancels phase distortions along the spectrum in order to determine the unknown phase of the pulse.

For every spectral component in the pulse the accompanying generated second harmonic electric field is

$$E(2\omega) = \int |E(\omega + \Omega)||E(\omega - \Omega)|e^{i[\phi(\omega+\Omega)+\phi(\omega-\Omega)]}d\Omega \quad (4)$$

with SHG intensity is given by $|E(2\omega)|^2$ and the total spectral phase can be written as $\phi(\omega) = \psi(\omega) + f(\omega)$, where $\psi(\omega)$ and $f(\omega)$ represent the unknown input laser phase and reference phase functions respectively. The reference function is chosen as $f(\omega) = \alpha \cos(\gamma\omega - \delta)$ where α is the amplitude, γ is the temporal duration and δ is the scanning parameter ensuring that reference function samples all the frequencies in the bandwidth [10]. A Taylor expansion of the phase term and neglecting third and higher order terms gives:

$$E(2\omega) \approx e^{2i\phi(\omega)} \int |E(\omega + \Omega)||E(\omega - \Omega)|e^{i[\frac{\partial^2\phi(\omega)}{\partial\omega^2}]}d\Omega \quad (5)$$

with the GDD = $\frac{\partial^2\phi(\omega)}{\partial\omega^2}$. The SHG is maximised when the GDD is zero, which leads to the condition to find spectral phase.

$$\frac{\partial^2\phi(\omega)}{\partial\omega^2} = \psi''(\omega) + f''(\omega) = 0 \quad (6)$$

$$\psi''(\omega) = -f''(\omega) = -\alpha\gamma^2 \cos(\gamma\omega - \delta) \quad (7)$$

From equation 7, the unknown phase which is the GDD can be determined. The MIIPS process is summarized in figure 1.

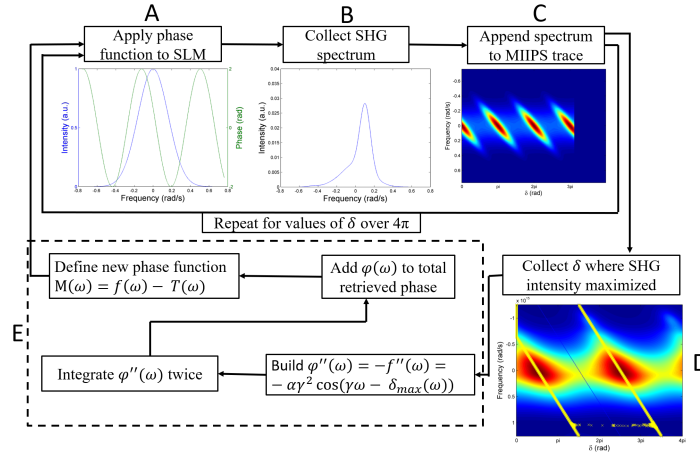


Figure 1: Schematic diagram of the MIIPS process. This include the definition and application of reference phase function onto the SLM (A), scanning over the laser pulse to measure the SHG for each spectral phase (B). The SHG spectrum is recorded (C) and the region where the scanning parameter δ is maximised is recorded (D). The process of retrieving the phase is summarized in section E.

3. Experimental setup

Figure 2 shows the setup used. A Ti:Sapphire femtosecond laser (Tsunami: Spectra-Physics) delivering pulses centred at 800 nm with a pulse duration of 90 fs and delivering energies of around 12 nJ was coupled into a highly nonlinear polarization maintaining all normal dispersion photonic crystal fiber (ANDi PCF) (NL-1050-NE PM, NKT Photonics) of approximately 14 cm in length. An ANDi PCF was used as a result of preliminary studies carried out in this type of fiber which showed that a coherent and flat-top spectra spanning over more than one octave can be generated over a wide range of pump pulse parameters. This earlier studies also showed the independence of coherence properties, spectral bandwidth and temporal compressibility on input pulse duration with the use of ANDi PCF [11, 12]. It is also established that the high peak power propagating in the micron sized PCF induces nonlinear effects. The two dominant processes are self phase modulation (SPM) and stimulated Raman scattering (SRS) within the fiber resulting in spectral broadening and the creation of a broadband supercontinuum light source [13].

Chirped mirrors were used in pre-compression before going into a pulse shaper consisting of two diffraction gratings (Thorlabs GR13-0608), two plano cylindrical lenses ($f = 250$ mm) and a 1-D computer addressable spatial light modulator (SLM)(Jenoptik S640d). The components were arranged in a $4f$ configuration similar to that outlined by Weiner et al [14]. A $100 \mu\text{m}$ β -barium borate (BBO) and recrystallized urea crystals were used to generate SH signals which were collected by a spectrometer (Avantes) after passing through a band pass emission filter (Thorlabs BG39) used to block the illumination light. Scanning was carried out using computer controlled piezo stages (Newport Agilis 25) with a discrete step size of $1.5 \mu\text{m}$ while detection was carried out in the transmission geometry. The generated supercontinuum is focused tightly onto the sample with a high NA objective (0.9). A z-scan MIIPS was also performed to determine the effect of the focal position in the sample on the MIIPS process.

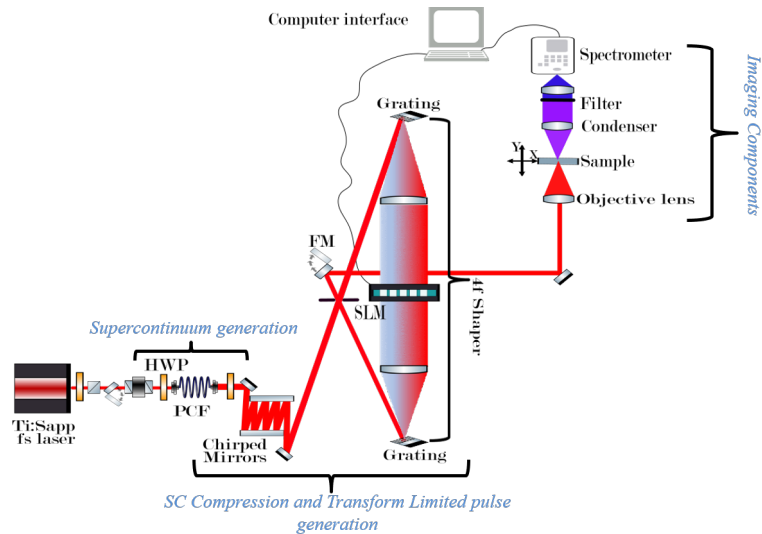


Figure 2: Schematic diagram of the experimental setup showing the region of supercontinuum generation, pulse characterization and compression as well as imaging configuration.

4. Results and discussion

From MIIPS theory, SHG is maximized when the quadratic phase of a laser pulse is zero (refer to equation 6). This implies for a compressed pulse, the total phase of the pulse within the SC region must be approximately zero. As seen from figure 3(a), the total phase (red line) is approximately flat within the SC spectrum (blue line) in accordance with MIIPS phases previously recorded [10, 15]. The phase is compensated to within 0.001 rad over the entire pulse bandwidth indicating that distortions introduced by the high-NA objective are well compensated [10]. This implies there is negligible phase difference between the spectral components. The GDD obtained from the retrieved phase, in frequency space, (black data points) is measured at a wavelength corresponding to the central excitation wavelength using a polynomial (from equation 3)(green line).

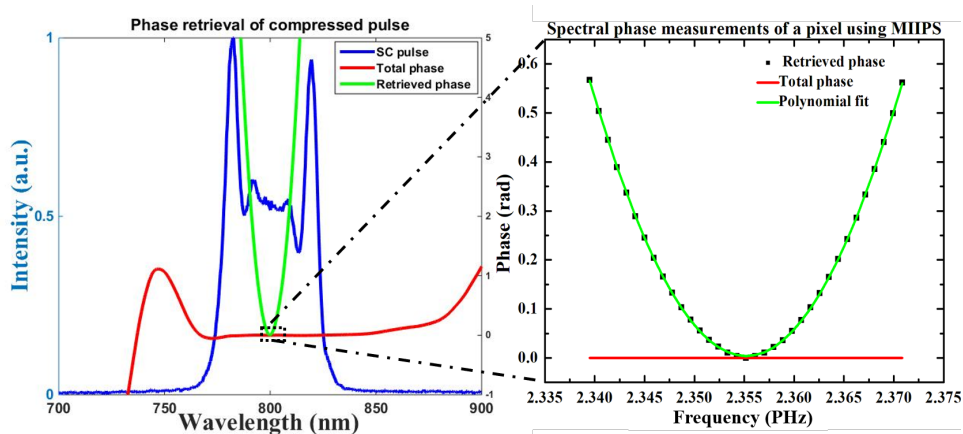


Figure 3: Spectral phase information obtained after MIIPS procedure.

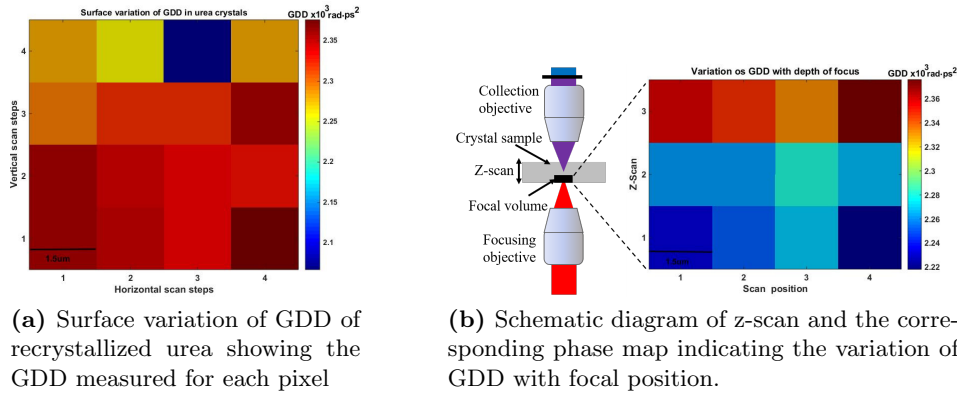
The polynomial parameters for figure 3 are summarized in the table 1 below.

The GDD value determined in this instance is 2.36×10^{-3} rad.ps². Coefficients of third and higher order terms are insignificant because MIIPS is only limited to the measurement of second

Table 1: Polynomial fit parameters.

Parameter	Value	Error	Interpretation
k_0 (rad)	0.0039	± 0.0004	Envelope of phase propagation.
k' (rad.ps)	-0.00116	± 0.00005	Temporal shift of propagating pulse.
k'' (rad.ps ²)	0.00236	± 0.00001	Group delay dispersion (GDD).

order polynomial coefficient [8]. Variation of GDD with scan position across recrystallized urea salt are shown in figure 4a. The GDD variation is as a result of the different urea thickness formed during recrystallization resulting in different optical path lengths.


Figure 4: Phase contrast maps of recrystallized urea and BBO.

As depicted in figure 4b, the focal position affects the GDD. This shows that unlike other techniques that permitted the measurement across the entire thickness of the sample [16, 17], the signal response from MIIPS depends on the focal position within the sample. The closer to the first surface the focus is, the smaller the GDD recorded which implies the pulse traverses a shorter distance thereby reducing the impact of GDD.

MIIPS phase contrast imaging: A potential application for this phase measurement technique is the possibility of implementing it in GDD (phase) contrast microscopy. Preliminary contrast imaging was conducted on recrystallized urea crystals and the $100\mu\text{m}$ β -barium borate (BBO) with camera images shown in figure 5. Phase contrast mapping generated via scanning a 5×5 grid in $1.5 \mu\text{m}$ steps is shown in figure 6 (a) and (b) respectively.

The GDD map of BBO shows an expected nearly constant GDD across the scan. In contrast to that of the BBO, the map of urea shows greater variation with a range from 1.5 to above 3.5×10^{-3} rad.ps² implying that for a non uniform sample, the extracted phase acquired through the MIIPS process is sensitive to position. These results indicate that MIIPS can offer a new complimentary technique to phase contrast microscopy.

5. Conclusion

We have demonstrated the working principle of MIIPS as a temporal pulse characterization technique and its potential use as a complimentary phase contrast imaging technique. Variation of GDD with depth of focus indicates compression using MIIPS is carried out in the focal volume

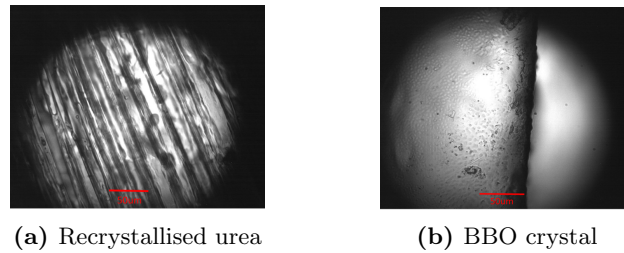


Figure 5: Bright-field micrograph of recrystallized urea and BBO

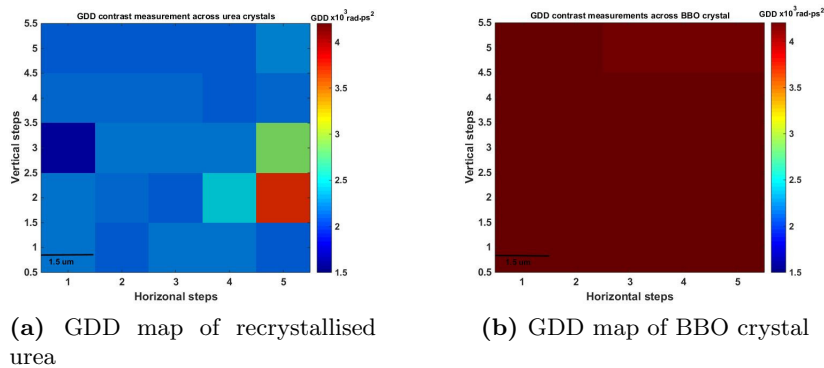


Figure 6: Phase contrast maps of recrystallized urea and BBO

of the focusing objective. This makes it possible to extract information from a specific area and depth within a given material. We have also seen that for a non uniform sample, the extracted phase acquired through the MIIPS process is sensitive to position, and therefore suggests phase contrast imaging is possible.

References

- [1] Trebino R 2000 *Frequency-Resolved Optical Gating: The Measurement of Ultrashort Laser Pulses* **Ed.1** (Springer US) ISBN 978-1-4613-5432-1
- [2] Iaconis C and Walmsley IA, 1998 *OPTICS LETTERS* **23** pp 792-794
- [3] Spangenberg D, Rohwer E, Brüggemann MH, and Feurer T 2015 *OPTICS LETTERS* **40** pp 1002-1005
- [4] Sukhoivanov I, Iakushev S, Shulika O and Lysak V 2007 *9th International Conf. on Transparent Optical Networks* Rome pp 128-131
- [5] Durst M, Kobat D and Xu C 2009 *Optics Express* **34** pp 1195-1197
- [6] Mak K, Travers J, Joly N, Abdolvand A and Russell P 2013 *Optics Express* **38** pp 1195-1197
- [7] Lozovoy V, Pastirk I and Dantus M 2004 *Optics Letters* **29** pp 775-777
- [8] Comin A, Ciesielski R, Piredda G, Donkers K and Hartschuh A 2014 *Journal of the Optical Society of America B* **31** pp 1118-1125
- [9] Tu H, Liu Y, Lægsgaard J, Turchinovich D, Siegel M, Kopf D, Li H, Gunaratne T and Boppart SA 2012 *Applied Physics B: Lasers and Optics* **106** pp 379-384
- [10] Xu B, Gunn J, Cruz J, Lozovoy V and Dantus M 2006 *Journal of the Optical Society of America B* **23** pp 750-759
- [11] Heidt A 2010 *Journal of the Optical Society of America B* **27** pp 550-559
- [12] Heidt A, Rothhardt J, Bartelt H, Rohwer E, Limpert J and Tünnermann A 2011 *Optics Express* **19** pp 13873-13879
- [13] Dudley J M, Genty G and Coen S 2006 *Reviews of Modern Physics* **78** pp 1135-1184
- [14] Weiner A M, 2000 *Review of Scientific Instruments* **71** pp 1929-1960
- [15] Comin A, Ciesielski R, Coca-López N and Hartschuh A 2016 *Optics Express* **24** pp 2505-2512
- [16] Rosker M J, Cheng K and Tang C L 1985 *IEEE Journal of Quantum Electronics* **21** pp 1600-1606
- [17] Tamošauskas G, Beresnevičius G, Gadonas D and Dubietis A 2018 *Opt. Mater. Express* **8** pp 1410-1418